Available online at www.sciencedirect.com
ScienceDirect
Cement and Concrete Research 37 (2007) 1418–1426
Cement and Concrete Research

Mechanisms and parameters controlling the tricalcium aluminate reactivity in the presence of gypsum

Hélène Minard, Sandrine Garrault *, Laure Regnaud, André Nonat

I.C.B., Institut Carnot de Bourgogne UMR 5209 CNRS-Université de Bourgogne 9 Avenue Alain Savary B.P. 47870-21078 DIJON CEDEX, France

Received 2 March 2007; accepted 1 June 2007

Abstract

To understand the mechanisms and the parameters controlling the reactivity of tricalcium aluminate in the presence of gypsum at an early age, a study of the hydration of the "C_3A–sulphate" system by isothermal microcalorimetry, conductimetry and a monitoring of the ionic concentrations of diluted system suspensions have been carried out with various gypsum quantities. The role of C_3A source and its fineness were also studied. This work shows the fast initial formation of AFm phase followed by ettringite formation during the period when the sulphate is consumed. It has been highlighted that the time necessary to consume all the gypsum varies with the type of C_3A and it has been attributed to the intrinsic reactivity of each one and mainly to the change of fineness from one C_3A to another. Results are discussed alongside hypothesis from the literature to explain the slowing down of C_3A hydration process in the presence of calcium sulphate.

Keywords: Hydration; Kinetics; Ettringite; $Ca_3Al_2O_6$

1. Introduction

Tricalcium aluminate (C_3A), which can constitute up to 15% of the Portland clinker, reacts very quickly with water to form calcium hydroaluminates, AFm phases of type that induce the stiffening of the paste. To avoid this phenomenon, calcium sulphate is added which leads to the formation of calcium trisulfoaluminate, ettringite ($Ca_6Al_3(SO_4)_3(OH)_{12}$, $26H_2O$) with a slower process. Therefore, the reactivity of the tricalcium aluminate-calcium sulphate system is of a very high importance since it can influence the workability of cement paste. Many hypotheses regarding the action of calcium sulphate have been suggested but the mechanisms by which it slows down the reaction of C_3A are not yet fully elucidated. Some authors evoke the formation of a barrier layer. According to them, the hydrated products form a more or less permeable layer on the C_3A surface that limit the transport of water and ions. Nevertheless, the defenders of this hypothesis disagree on the nature and the composition of this layer: the product could be crystalline [1–3] or non-crystalline calcium sulfoaluminate layer [4–6], or for others, crystallinity depends on pH [5]. It was also suggested that it could be calcium hydroaluminate precipitating in the same time than ettringite that could decelerate C_3A hydration [7].

Other authors consider the adsorption of the sulphate on C_3A [8,9]. The sulphate ions would block therefore the active sites of the dissolution and would contribute to the decrease of the dissolution rate of C_3A. Such disagreements in the interpretations of the experimental data are probably due to the fact that most of the phenomena occur at a very early age, even during mixing. Moreover, results are strongly dependent on the experimental conditions which are not always perfectly controlled. In particular, making a paste with two very reactive powders and a small amount of water inevitably introduces local heterogeneities. So, more work is required to understand the reactivity and the kinetics of the C_3A–$CaSO_4$–H_2O mix. In the present work, to avoid the heterogeneity problems, we chose to work with stirred diluted suspensions. Indeed, this procedure has been found very efficient to understand the mechanisms and the parameters controlling the reactivity of tricalcium silicate at an early age. In addition, it is very easy, in these conditions, to follow the evolution of the liquid phase which is the medium for exchange of matter between solids during the

* Corresponding author.
E-mail address: sandrine.garrault@u-bourgogne.fr (S. Garrault).

0008-8846/$ - see front matter © 2007 Elsevier Ltd. All rights reserved.
doi:10.1016/j.cemconres.2007.06.001

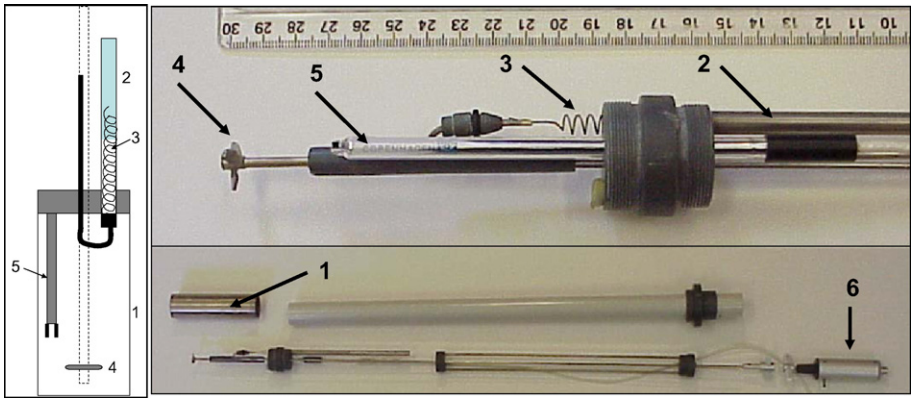

Fig. 1. Calorimetric cell (1); solid is placed in the tube (2) before experiment and introduced in the cell by mean of the spring (3); stirrer (5); stirring motor (6); conductivity cell (5).

reaction. The overall reaction has been followed by isothermal microcalorimetry according to the procedure developed to study C_3S hydration [10]. In parallel, the same experiments have been performed in conductimetry cells allowing sampling at different hydration times for solid and liquid phase analysis.

Different parameters were studied such as the C_3A source and fineness, because of the importance of grain size on reactivity, and the gypsum amount with the objective to identify and quantify the first hydration products in order to evaluate their eventual impact on the kinetics of C_3A hydration.

2. Materials and methods

The hydration of C_3A was followed at 25 °C with a high sensitivity (0.1 μW) isothermal Tian–Calvet type microcalorimeter (SETARAM M60) in diluted suspension which is associated with a conductimetric system. The calorimetric cell was built on the same principle as that described by Damidot and al. [10] but with a bigger cell (50 mL instead of 10 mL) (see Fig. 1). Before starting the experiment, 50 mL of solution was introduced in the cell (1) with the appropriate amount of solid gypsum and 2 g of C_3A (7.4 mmol) was placed in the tube (2).

The calorimetric cell is then introduced in the calorimeter and the stirring (4) of the solution begins; once the thermal equilibrium is reached (about 2 h), C_3A is introduced in the cell by means of the spring (3). Both heat flow and conductivity (measured by a conductivity cell (5)) evolutions were obtained as a function of time. The thermal inertia of such a calorimeter is relatively high. If the thermal event is shorter than the time constant of the calorimeter, while the total heat is correct, the intensity of the observed signal is smaller and its duration is greater than those of the true event (Fig. 2). The true signal, corrected from the transfer function of the calorimeter, was obtained from a one step Fourier filter. The transfer function of the calorimeter was estimated from the heat liberated by passing an electric current of 30 mW during 5 s.

The same experiments as those performed in the calorimeter were reproduced in a temperature controlled (25 °C) reactor (25 g of C_3A −250 mL of solution) equipped with a conductivity cell. Recording the electrical conductivity of the solutions in both experiments allows their synchronisation. The chemical composition of the liquid phase was studied by taking a few millilitres of solution at several times; each solution was filtered (0.3 μm, Millipores) and a small known quantity of hydrochloric acid was added. Calcium and aluminium concentrations were checked by Spectrometric Atomic Absorption (Perkin-Elmer, model 3030) and sulphate concentrations by ionic chromatography (Dionex).

The solid part was washed with pure alcohol in order to analyse solids by X-ray diffraction (Inel CPS 120) and the products were observed by SEM (Jeol, model 6400F).

Three different «batches» of cubic C_3A, L1, L2 and C respectively, were used to carry out the experiments on the hydration of C_3A in the presence of gypsum and also of lime to be closed to hydration in paste for which the solution is quickly saturated with respect to calcium hydroxide; samples L1 and L2 were supplied by Lafarge LCR and sample C was supplied by CTG Italcementi. Their particle size distribution has been determined and represented as the percentage volume of particles versus median diameters in Fig. 3. Their specific surfaces, determined by Blaine's method, were respectively 3700 cm^2/g, 3250 cm^2/g and 3300 cm^2/g.

These experiments were performed with 1 g (3.7 mmol) of C_3A and the amount of gypsum varied from an experiment to another: they are expressed in moles and percentage mass of gypsum in Table 1.

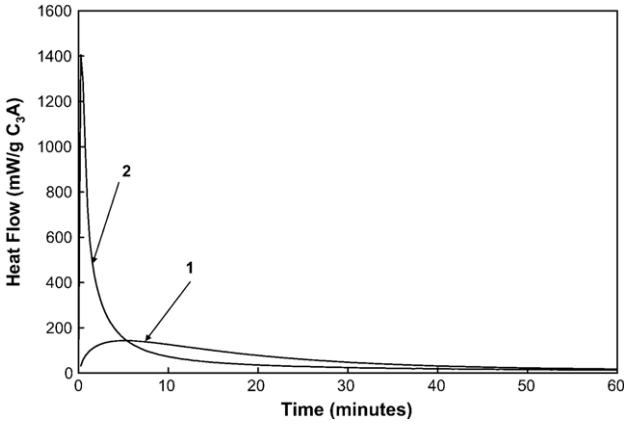

Fig. 2. (1) Heat evolution rate curve recorded from the calorimeter observed signal. (2) True signal obtained after correction of (1) with a one step Fourier filter.

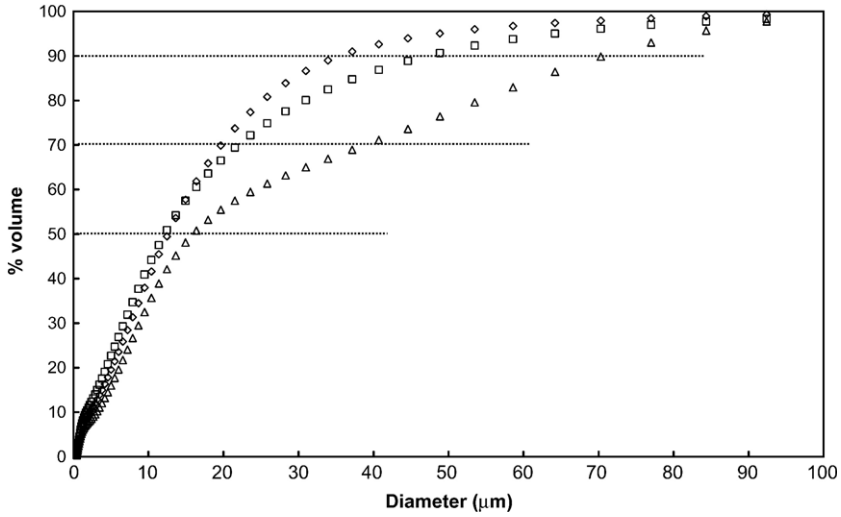

Fig. 3. % volume of particles versus median diameters for C_3A L1 (□), C_3A L2 (◇) and C_3A C (△) determined by laser scattering particle size distribution analyzer. D_{50}=12.5 μm for C_3A L1 (□) and C_3A L2 (◇) and D_{50}=16.4 μm for C_3A C (△). D_{70}=19.6 μm C_3A L2 (◇), D_{70}=21.5 μm for C_3A L1 (□) and D_{70}=40.7 μm for C_3A C (△). D_{90}=37 μm C_3A L2 (◇), D_{90}=49 μm for C_3A L1 (□) and D_{90}=70 μm for C_3A C (△).

C_3A (L2) was also used to prepare samples of different grain sizes: a mix of 30 g of C_3A (L2) was mixed in an inert solvent, absolute ethanol, submitted to a high dispersive treatment (ultrasound 30 s) and poured in a long tube (1 m long, 2 cm in diameter). The suspension was left to stand for one month. After complete sedimentation, the solvent was then eliminated and the sediment dried. The sediment was separated to obtain C_3A slices with different diameters from the finest particles on the surface to the biggest in the bottom numerated from 1 to 11.

The median diameter of particles of each bracket was measured by laser granulometry (Fig. 4). It varies from 1 to 62 μm.

Pure gypsum from Merck was used. Lime was obtained by decarbonation overnight at 1000 °C of calcium carbonate provided by Aldrich.

Table 1
Gypsum quantities used in experiments expressed in moles and percentage mass of gypsum from different batches: L1, L2 and C

Experiments	Gypsum quantity (mmol)	Percentage mass of gypsum
L1a	0.35	6
L1b	0.58	10
L1c	0.87	15
L1d	1.16	20
L1e	1.74	30
L1f	2.50	43
L2a	0.13	2.1
L2b	0.38	6.1
L2c	0.63	9.7
L2d	1	14.7
L2e	1.50	20.5
L2f	1.88	24.4
L2 g	2.50	30.1
Ca	0.38	6.1
Cb	0.75	10.25
Cd	1.13	15.44
Cf	1.50	20.5

3. Results

3.1. Heat flow, conductivity and ionic concentrations evolutions during hydration of C_3A–gypsum mix

Fig. 5 shows the evolution of the experimental heat flow, after correction of the inertia by the one step Fourier filter, and conductivity of the solution recorded during the hydration of 7.4 mmol of C_3A (from batch C) and gypsum (1.5 mmol; gypsum/C_3A molar ratio=0.2) in 50 mL of a solution saturated with respect to portlandite (L/S=25). Under these conditions all the gypsum was not initially dissolved: the solution becomes saturated with respect to gypsum when 0.625 mmol is dissolved. It remains 0.875 mmol solid gypsum in the initial suspension before C_3A is added. The heat evolution rate curve shows two main exothermic peaks due to very fast events; the first is very sharp. The peaks appear to be composed of several ones. The evolutions during hydration of the corresponding ionic concentrations are represented in Fig. 6 with the electrical conductivity of the solution.

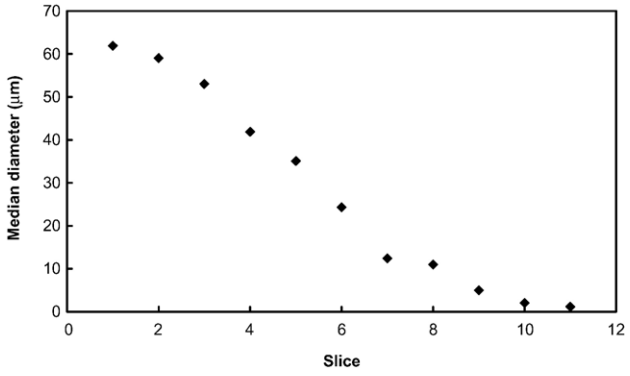

Fig. 4. Median diameters for the different brackets of tricalcium aluminate grains obtained after settling in ethanol and separation. The grain size was determined by laser scattering particle size distribution analyzer.

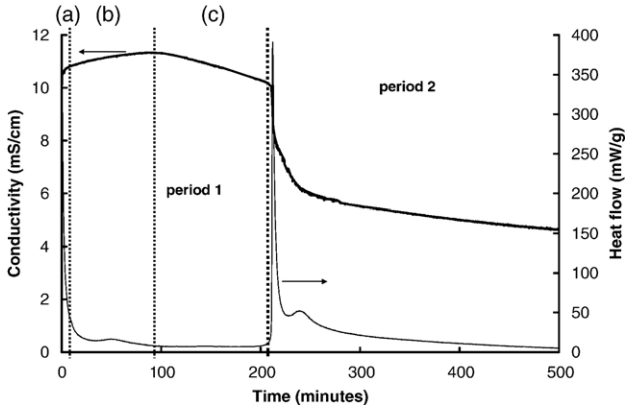

Fig. 5. Heat flow corrected from calorimeter inertia and conductivity evolutions during hydration of 7.4 mmol of C_3A (batch C) and gypsum (1.5 mmol) in 50 mL of a solution saturated with respect to the portlandite (L/S=25).

In the following discussion, a distinct period is arbitrarily associated with each peak and to the weak thermal activity which follows it. As one can note in Fig. 6, period 1 corresponds to the presence of sulphate ions in solution; it refers to the period of calcium sulphate consumption and ettringite formation. The initial sulphate concentration corresponds to the solubility of gypsum in a saturated solution with respect to portlandite which is 2.15 g/L or

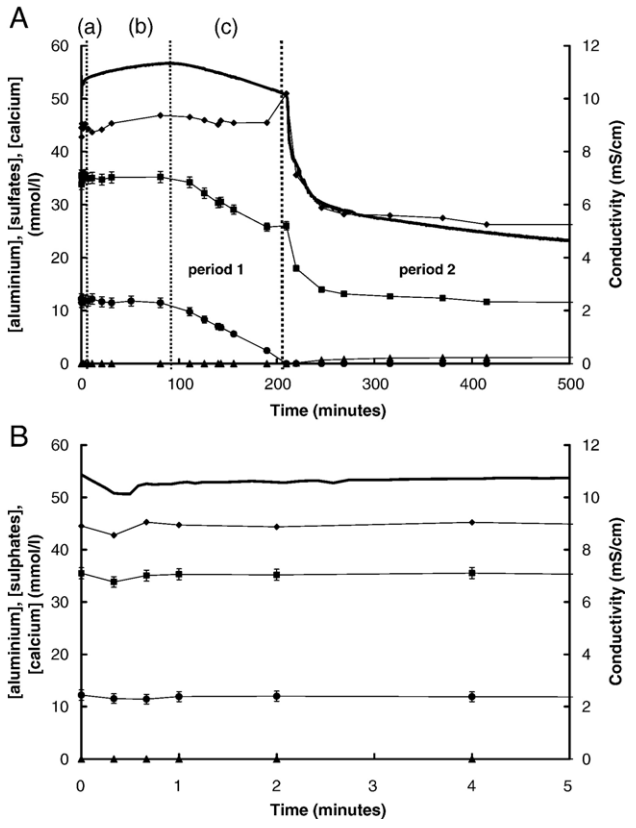

Fig. 6. (A) Ionic concentrations (aluminium: ▲, sulphates: ●, calcium: ■ and calculated hydroxide: ◆) and conductivity evolutions during hydration of 7.4 mmol of C_3A (batch C) and gypsum (1.5 mmol) in 50 mL of a solution saturated with respect to the portlandite (L/S=25). (B) Ionic concentrations evolution during the first 5 min of hydration of 7.4 mmol of C_3A (C) and gypsum (1.5 mmol) in 50 mL of a solution saturated with respect to portlandite (L/S=25).

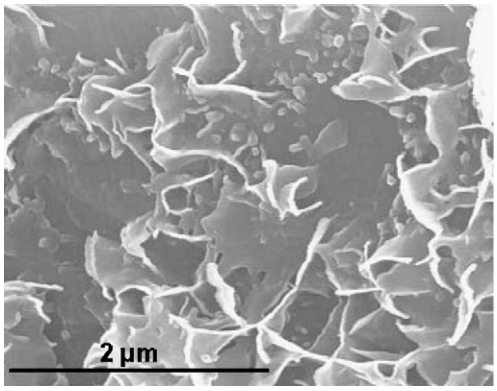

Fig. 7. Micrograph of a grain of C_3A hydrated during 3 min in a solution saturated with respect to calcium sulphate and calcium hydroxide.

12.5 mmol/L. Period 2 begins when all the sulphate ions have been entirely consumed and then the second exothermic peak appears.

Period 1 can be broken down into 3 stages as follows:

- stage (a) corresponds to the first 5 min of the C_3A hydration in the presence of gypsum and calcium hydroxide, it presents a short and very intense exothermic peak, with an intensity about 1400 mW/g of C_3A. The hydroxide concentration (deduced from the electroneutrality relation) and conductivity follow exactly the evolution of the sulphate and calcium concentrations: a slight fall is observed in the first minute of the hydration (Fig. 6B). The scanning electron micrograph presented in Fig. 7 shows a grain of C_3A hydrated during this stage (hydration stopped after 3 min). The surface of the C_3A grains is covered by two types of hydrates with different morphologies: small ettringite needles and sheets of AFm phase, the latter being dominant.
- stage (b) corresponds to the period during which the sulphate concentration increases despite the fact that this species is being consumed for the formation of ettringite. In fact, as all ions consumed by the reaction to form ettringite are replaced by the dissolution of an equivalent amount of gypsum, a quasi-stationary state is established. During this stage b, there always remains solid gypsum in equilibrium with the solution (Fig. 8). From the kinetic point of view, the rate of heat evolution curve (Fig. 5) shows, after the decrease of the initial peak, a new exothermic peak centred over the period (b) and a constant flow over the period (c).
- the stage (c) coincides with the quasi-linear decrease of the sulphate concentration until the complete disappearance of this ion. The calcium concentration decreases also continuously.

The aluminium concentration is lower than the practical limit of detection of the analytical method for all the periods except for the first point at 15 s when it is about 10 µmol. At the end of the stage c, ettringite is the dominating hydrated phase.

The beginning of period 2, after the exhaustion of the sulphate ions, coincides with a strong renewal of thermal activity. At the beginning of this period, Fig. 5 shows a peak whose intensity in the case of this experiment is about 400 mW/g C_3A corresponding to a very fast exothermic reaction. The calcium concentration increases

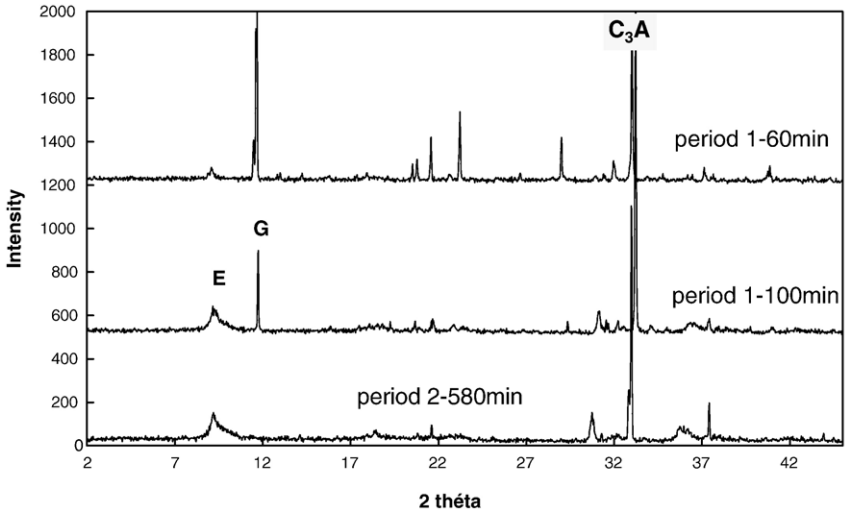

Fig. 8. X-ray diffraction patterns obtained during hydration of 7.4 mmol of C_3A (batch C) and gypsum (1.5 mmol) in 50 mL of a solution saturated with respect to the portlandite (L/S=25). E=Ettringite, G=gypsum.

simultaneously with the exhaustion of the sulphate ions in solution, then decreases. The aluminium concentration is not zero; it increases progressively. At the end of the experiment, C_3A and ettringite are still present (Fig. 8).

3.2. Influence of gypsum initially introduced during the tricalcium aluminate hydration

The influence of the initial amount of gypsum was studied on the different stages of hydration of C_3A. These experiments were performed with C_3A (L1), (L2) and (C). In all experiments 1 g (3.7 mmol) of C_3A was used and the amount of gypsum varied from an experiment to another: they are expressed in moles and percentage mass of gypsum in Table 1. These experiments take place always with a solid gypsum reservoir except experiment L2a in which only a saturated solution is used. Experimental heat evolution rate curves recording during hydration of C_3A (L2) carried out with various amounts of gypsum are reported on Fig. 9.

The beginning of all the heat evolution rate curves is superposed whatever the amount of gypsum. The amount of gypsum does not have any effect on the beginning of the hydration.

The time of occurrence of the second exothermic peak, i.e. the time needed to consume all gypsum, increases with the gypsum quantity. This time is plotted on Fig. 10 as a function of gypsum percentage in the mix C_3A/gypsum for each C_3A.

The hydration of C_3A L1 is faster than others. In addition, for each type of C_3A, the time necessary to exhaust the totality of the sulphate ions does not evolve in a linear way with the quantity of gypsum initially introduced.

The conductivity evolutions obtained during hydration of two types of C_3A, L2 and C, with the same amount of gypsum are compared in Fig. 11. The shape of the electrical conductivity considerably varies with the C_3A source. The time necessary to consume all the gypsum which corresponds to the vertical drop of the electrical conductivity as seen Figs. 5 and 6 depends

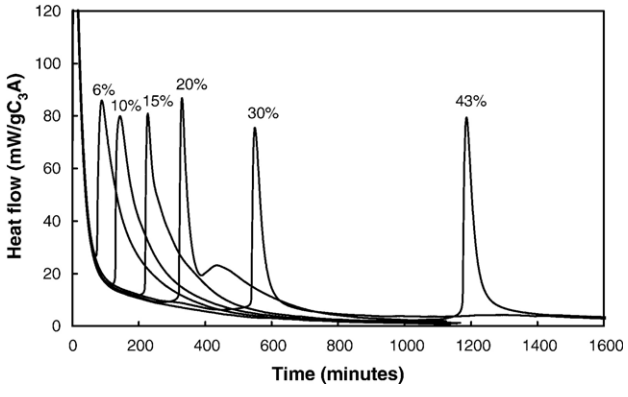

Fig. 9. Heat evolution rate curves during the hydration of C_3A (L1) in solutions saturated with respect to portlandite (L/S=25) carried out with increasing quantities of gypsum.

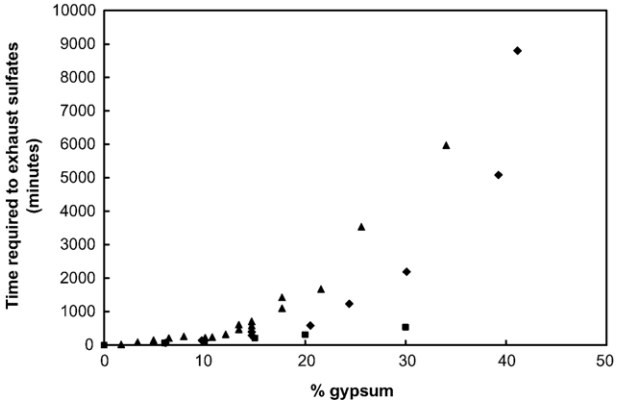

Fig. 10. Time necessary to consume all sulphate ions versus percentage of gypsum introduced in the mix C_3A/gypsum for experiments detailed in Table 1; C_3A L1 (■), C_3A L2 (◆) and C_3A C (▲).

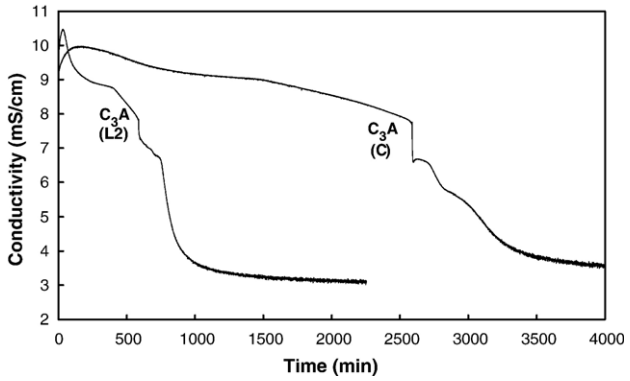

Fig. 11. Evolution of the electrical conductivity of the solutions during hydration of 7.4 mmol of C_3A (L2 and C) and gypsum (3 mmol) in a solution saturated with respect to the portlandite (L/S=25).

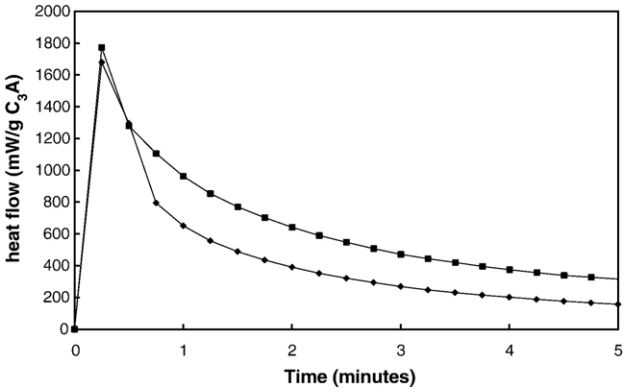

Fig. 13. Heat flow variation during the first 5 min of hydration of C_3A (2 g, batch C) in a solution saturated with respect to portlandite (◆) and in a solution saturated with respect to portlandite containing gypsum (1.25 mmol) (■) (L/S=25).

strongly on the C_3A batch. Period 1 lasts only 585 min in the case of C_3A (L2) whereas it lasts 2585 min in the case of C_3A (C). The initial evolution of conductivity is also different. For C_3A (L2), conductivity increases to 10.45 mS/cm in 38 min whereas the conductivity increases only to 9.98 mS/cm in 170 min for C_3A (C).

3.3. Influence of granularity on C_3A hydration

Two extreme slices of C_3A L2 with very different particle sizes were used: slice 3 and slice 11 for which the particle median diameters are 53 μm and 1.2 μm respectively.

The shape of the heat evolution rate and electric conductivity curves varies considerably with the C_3A granularity (Fig. 12). The time necessary to exhaust the same amount of gypsum depends on the size of the C_3A particles. Period 1 of ettringite formation lasts only 486 min in the case of the section of median diameter equal to 1.2 μm whereas it lasts 11430 min in the case of the section centred on 53 μm. The initial evolution of conductivity is also different according to the particle size of the C_3A. A strong increase in conductivity takes place in the case of the sample centred around 1.2 μm ($\Delta\gamma$=1.12 mS/cm) whereas the increase in conductivity is very weak ($\Delta\gamma$=0.15 mS/cm) in the case of the largest particles of C_3A.

Considering the maximum intensity of second exothermic peak, it is 30 times larger in the case of the smaller particles than in the case of the largest section.

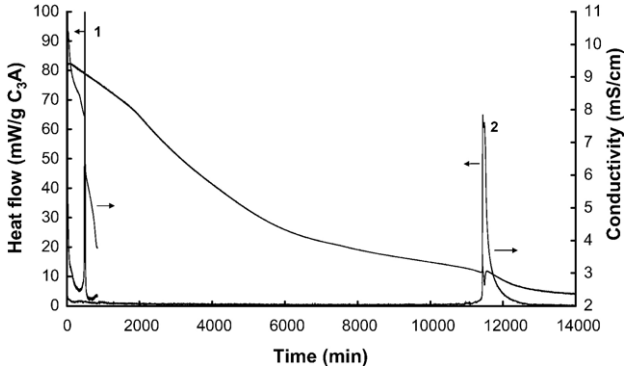

Fig.12. Heat flow and conductivity evolutions during hydration of 7.4 mmol of C_3A (resulting from batch L2) with two different granularity (1: slice 11 median diameter of 1.2 mm and 2m and 2: slice 3 median diameter of 53 μm) and gypsum (3.75 mmol) in a solution saturated with respect to the portlandite (L/S=25).

4. Discussion

4.1. Reaction sequences

As previously seen, two periods can been distinguished, a first corresponding to sulphate consumption that is to say to the formation of ettringite, and another when there is no sulphate in solution.

4.1.1. Period 1

The period 1 has been detailed in three stages. During the stage a, corresponding to the very first minutes of hydration, as the aluminium concentration is zero, it indicates that all the ions provided by dissolution of the C_3A have precipitated immediately. After 3 min, ettringite is present on the surface of C_3A grains and AFm also appears in the form of "sheets", this one being predominant.

The initial reduction in sulphate and calcium concentrations shows that the rate of their consumption is transitorily higher than the rate of gypsum dissolution. The consumption of calcium sulphate can be due to the precipitation of ettringite, the precipitation of AFm monosulphate, or to the adsorption on the C_3A as was suggested in a previous work. Fig. 13 compares the heat flows released during the first 5 min of the hydration of C_3A in a saturated lime solution and in a saturated lime solution with an excess of gypsum respectively, all other conditions being equal. The first two recorded values are identical, then, after 45 s, heat flow is systematically weaker in the presence of gypsum. It can be assumed that during the thirty first seconds, phenomena which take place with or without gypsum are the same: dissolution of the C_3A and the quasi-instantaneous precipitation of AFm.

Relative amount of AFm and ettringite is difficult to quantify but microscopy seems to show that after 3 min AFm remains preponderant. During period b, a quasi-stationary state is

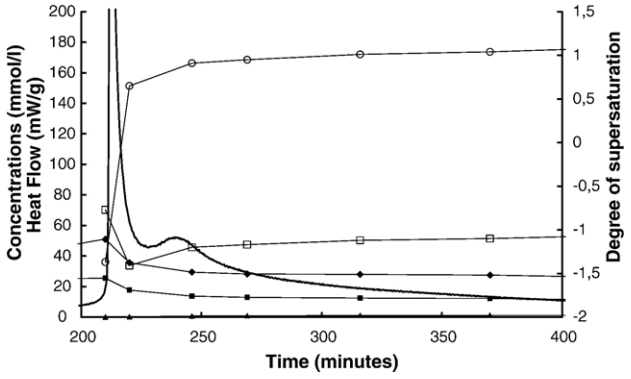

Fig. 14. Heat flow, ionic concentrations (aluminium: ▲, sulphates: ●, calcium: ■ and calculated hydroxide: ◆) and degree of supersaturation with respect to ettringite (□) and to monosulfoaluminate(○) evolutions during hydration of 7.4 mmol of C_3A (resulting from a batch C) and gypsum (1.5 mmol) in 50 mL of a solution saturated with respect to the portlandite (L/S=25).

established, where all calcium and sulphate ions consumed by ettringite formation are replaced by gypsum dissolution. The concentrations of sulphate and calcium which are established in the "stationary" state were surprisingly very closed to the gypsum solubility. The dissolution of the gypsum is then not a limiting step.

A slight increase of conductivity is however noticed due to the increase of hydroxide concentration. This could be explained by the exchange of two hydroxide ions of AFm by one sulphate as indicated by reaction (1):

$$Ca_xAl_2(OH)_{(2x+6)}+ySO_4^{2-} \rightarrow Ca_xAl_2(OH)_{(2x+6-2y)}(SO_4)_y+2yOH^-. \quad (1)$$

This could also explain the very slight decrease of sulphate concentration during this same period.

The second exothermic peak centred over the period (b), near 50 min in Fig. 4 represents, assuming a constant heat of reaction, an increase of the hydration rate over the period (b). It could be interpreted as the acceleration of ettringite formation which would follow a classic process of nucleation and growth.

During period c, it is interesting to note that the linear decrease of the sulphate concentration corresponds to a period of constant flow, i.e. a constant reaction rate. Assuming that the heat of formation of the ettringite from C_3A and gypsum is equal to −452 kJ/mol [12], during the stage (c) the rate of formation of the ettringite is $0.03.10^{-6}$ mol/s, it corresponds to a rate of sulphate consumption of $0.090.10^{-6}$ mol/s. The rate of sulphate concentration variation for this period, obtained from solution analysis (Fig. 5), is 11.5/6720 mmol per litre and second, that corresponds to the very similar value of $0.085.10^{-6}$ mol/s in the 50 mL of the experiment. So, during this period, there is only a consumption of sulphate ions from the solution, the reduction in the sulphate concentration in solution is thus due to the fact that all the solid gypsum was consumed in the stage (b).

4.1.2. Period 2

In the experimental conditions considered here (see Fig. 5), period 2 begins after 200 min of hydration with a second very sharp exothermic peak.

Fig. 14 shows the details of the ionic variations and the degrees of supersaturation of the solution with respect to ettringite and to calcium monosulfoaluminate during this period. The index of supersaturation was calculated according to SI=Log β, β being the ratio between the activity products in solution and the solubility product. They were obtained using the PHREEQC software with an extended Debye–Hückel approximation for activities and the solubility constants from Damidot [11]. The first negative values indicate that solution is undersaturated with respect to monosulfoaluminate calcium, consequently, one cannot ascribe the exothermic peak to the fast transformation of ettringite to monosulfoaluminate contrary to what is often advanced in the literature [12,9]. This strong exothermic resultant peak can only be attributed to the dissolution of C_3A. In fact the solution is very undersaturated with respect to C_3A which dissolves until the solution becomes supersaturated with respect to AFm which then precipitates. This step of pure dissolution of C_3A is very short which is why the thermal peak is very narrow. It is also seen in Fig. 12, the transient peak in the conductivity curve corresponds to the hydration of the coarser C_3A. But the thermal peak is also very intense, that is to say the dissolution rate of C_3A is very high; that means that ettringite and other hydration products do not limit the dissolution of C_3A. The solution is then free from sulphate ions; it is a solution for which the concentration is close to the solubility of the portlandite. Very quickly, the dissolution of C_3A in such a solution leads to the precipitation of calcium hydroaluminates, consuming calcium ions and releasing from the aluminium ions in solution which induces the strong fall of conductivity (Fig. 5) at this moment. Later, an exothermic peak of less intensity takes place followed by a relatively weak thermal activity. The calcium and aluminium concentrations do not evolve a lot. Impoverishment of the calcium ion concentration in solution (due to the precipitation of the calcium hydroaluminates) results in precipitation of calcium monosulfoaluminate which becomes more stable from a thermodynamic point of view than ettringite which dissolves (Fig. 14); it is a very slow transformation. After 2 days of hydration of C_3A under the above experimental conditions, ettringite in the form of needles and calcium monosulfoaluminate in the form of hexagonal plates cohabit, ettringite did not completely disappear (Fig. 15).

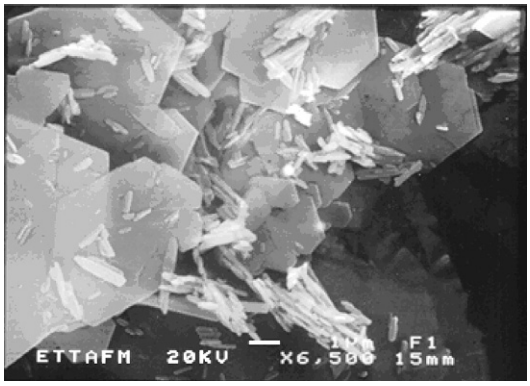

Fig. 15. Micrograph of a C_3A grain hydrated during two days in the presence of calcium sulphate, L/S=25.

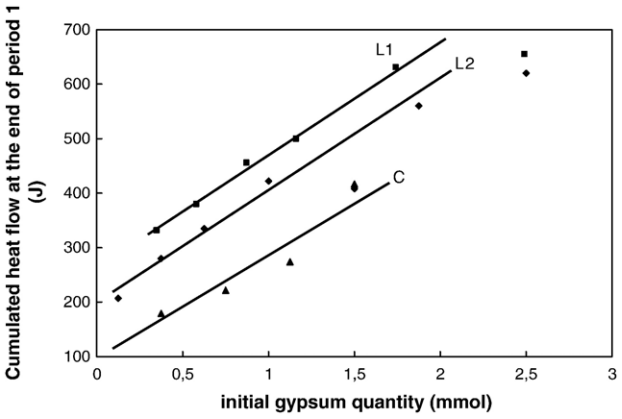

Fig. 16. Cumulated heat flow when all sulphates are consumed versus initial gypsum quantity obtained during hydration of 7.4 mmol of C_3A (resulting from various batches) and gypsum in a solution saturated with respect to the portlandite (L/S=25).

4.2. Estimation of the amount of AFm precipitated at early age

The integration of the rate of heat evolution curves obtained in the case of C_3A (L1) hydration with various quantities of gypsum leads to cumulative flows. The total heat released when the sulphate is exhausted is reported as a function of the initial gypsum quantity in Fig. 16, curve L1.

There is a linear relation between the quantity of heat released (Q) at the time when the gypsum is exhausted and the quantity of initial gypsum introduced (n_{gypsum}). The linear regression gives:

$$Q = 200^{*}n_{gypsum} + 272 (\text{Q in J and } n \text{ in mmol}).$$

Assuming that all the gypsum is only consumed by the precipitation of ettringite, the released heat after sulphate exhaustion is equivalent to a heat which can be written:

$$Q = (200^{*}3)^{*}n_{ettringite} + 272.$$

The slope of this line, 600 kJ/mol of formed ettringite, is, the ΔH of the equation:

$$Ca_3Al_2O_6 + 3CaSO_4,\ 2H_2O\ +\ 30H_2O \rightarrow Ca_6Al_2(SO_4)_3(OH)_{12},26H_2O.$$

The computed value of stet ΔH from the data available in the thermodynamic tables and reported by Taylor is −452 kJ/mol [13] which is in the same order of magnitude.

In addition, the y-intercept is equal to 272 J/g C_3A. This intercept occurs independently of the quantity of added gypsum. This can be attributed to the calcium aluminate hydrate precipitation observed. In such a case, the calcium aluminate hydrate quantity is independent of initial gypsum quantity.

The same representations are reported for the other C_3A on the same graph (Fig. 16). In all cases, a linear law between the quantity of released heat at the time when the gypsum is exhausted and quantity of initial gypsum introduced is observed. The same slope is obtained for all curves, of course the heat of C_3A hydration does not depend on the experimental conditions, but the y-intercept is different: for C_3A (L2), the value is 200 J/g C_3A (L2) and for C_3A (C), the value is 99 J/g C_3A (C). This indicates that the amount of calcium aluminate hydrate which precipitates at the very beginning of reaction depends on the type of C_3A that is used in the experiment. Although such experiments were not performed with different granulometric slices of a same C_3A, it seems that the finer the particles, the larger is the initial amount of AFm: the C_3A (L1) has the highest Blaine surface. Moreover in the case of very different particle size, there is a difference concerning the initial evolution of conductivity: a strong increase of 1.12 mS/cm is obtained for the smaller grains if it is compared with the value of 0.15 mS/cm observed with larger grains. If it is considered that this increase is due to the exchange hydroxide–sulphate ions in AFm, this is in agreement with the fact that there is more AFm precipitated when the C_3A has a larger surface area.

4.3. Kinetics of C_3A–gypsum hydration

Fig. 12 shows that the time necessary to exhaust the same quantity of gypsum drastically increases with the particle size of C_3A. The surface of 1 g of C_3A grains can be calculated with the hypothesis that the tricalcium aluminate grains are spherical with a diameter which is the median diameter of the considered section. The calculated surface obtained for grains with a diameter of 1.2 μm is 45 times greater than those obtained for diameter of 53 μm (1.6 m^2 against 0.036 m^2). Considering the time necessary to consume all sulphate, it is then possible to calculate the rate of gypsum consumption per surface unit: a value of 0.34 μmol min^{-1} m^2 is found for the bigger C_3A grains and 0.64 μmol min^{-1} m^2 for smaller one. The same order of magnitude is found which indicates that the rate of reaction seems to be controlled by the surface of C_3A.

Fig. 17 presents the percentage of C_3A consumed versus time necessary to exhaust sulphate in different cases. With very fine particles, the time necessary to consume all gypsum is reduced

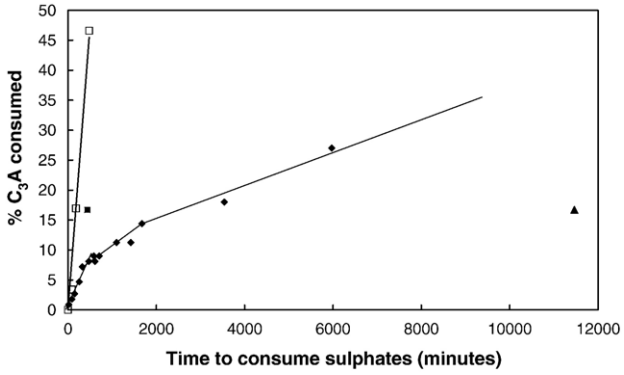

Fig. 17. Percentage of C_3A consumed in the mix C_3A/gypsum versus time necessary to consume all sulphate ions for the different experiments carried out with complete C_3A L2 (◆) and with C_3A L2 slice 10 (D_{50}=3 μm) (□). Results obtained on Fig. 11 are also reported: experiments with C_3A (resulting from batch L2) with two different granularities (■: slice 11 median diameter of 1.2 μm and ▲: slice 3 median diameter of 53 μm).

and with small monodispersed grains, gypsum is consumed at constant rate; the C_3A hydration rate is then constant.

With the polydispersed C_3A, the variation is not linear. It can be explained by the large C_3A granulometric distribution; the finest part hydrating faster than the coarsest parts.

These results can be linked to the differences observed between different C_3A. The fact that the time necessary to consume all gypsum varies with the type of C_3A (Figs. 10 and 11) can be attributed to intrinsic reactivity of each one and mainly to the change of accessible surface from one C_3A to another. The hydration of C_3A C is slower than others and it contains bigger grains (Fig. 3).

4.4. Mechanism of retardation of hydration in the presence of gypsum

The formation of ettringite cannot be at the origin of the retardation of hydration in the presence of gypsum otherwise on the one hand, the reaction rate would not be constant according to the quantity of ettringite formed contrary to what it is observed with small homodispersed grains in Fig. 17. On the other hand, the rate of dissolution of C_3A would not be so high when all the sulphate is consumed. The hypothesis of the formation of ettringite barrier that would limit the reaction rate is not valid and SEM images also show not much ettringite on C_3A surface.

The initial formation of AFm cannot either explain why the reaction rate decreases. Without gypsum, in calcium hydroxide solutions, the same product is formed, but the C_3A continues to react very quickly. Moreover, the finer the C_3A, the greater the quantity of precipitated AFM but the shorter the time to exhaust the sulphates.

The most plausible explanation of the slowing down of the rate of reaction of C_3A in the presence of calcium sulphate is the specific adsorption of the calcium and/or sulphate ions on the surface of the grains of C_3A which block dissolution sites of C_3A. This adsorption mechanism can explain the high C_3A dissolution rate which is observed during the second period of hydration when there is no sulphate ion.

5. Conclusion

These studies on the hydration of the tricalcium aluminate in the presence of gypsum show the formation of two different hydrates during the period when sulphates are present: ettringite as expected but also AFm phase at the very beginning.

The relative amount of AFm and the rate of formation of ettringite mainly depend on the specific surface of C_3A. However neither of these phases plays a barrier role to limit the hydration rate of C_3A. The slow process of ettringite formation could be limited by ettringite growth rate but its dependence on the surface area of C_3A indicates rather that it is limited by the dissolution of C_3A. The high C_3A dissolution rate which is observed after the disappearance of sulphate ions in solution supports this hypothesis that the adsorption of sulphate ions on C_3A is directly responsible for the retardation of hydration.

References

[1] M. Collepardi, G. Baldini, M. Panri, M. Corradi, Tricalcium aluminate hydration in the presence of lime, gypsum or sodium sulfate, Cem. Concr. Res. 8 (1978) 571–580.
[2] R. Holly, H. Peemoeller, M. Zhang, E. Reardon, C.M. Hansson, Magnetic resonance in situ study of tricalcium aluminate hydration in the presence of gypsum, J. Am. Ceram. Soc. 89 (3) (2006) 1022–1027.
[3] J. Pommersheim, J. Chang, Kinetics of hydration of tricalcium aluminate in the presence of gypsum, Cem. Concr. Res. 18 (6) (1988) 911–922.
[4] K. Scrivener, P.L. Pratt, Microstructural studies of the hydration of C_3A and C_4AF independently and in cement paste, in: F.P. Glasser (Ed.), Bristish Ceramic Proceedings, 1984.
[5] J.E. Bailey, D. Chescoe, A Progress Report on Analytical Electron Microscopy Studies of the Hydration of Tricalcium Aluminate, 595–598.
[6] J. Havlica, D. Roztocka, S. Sahu, Hydration kinetics of calcium aluminate phases in the presence of various ratios of Ca^{2+} and SO_4- ions in liquid phase, Cem. Concr. Res. 23 (2) (1993) 294–300.
[7] P.W. Brown, L.O. Libermann, G. Frohnsdorff, Kinetics of the early hydration of tricalcium aluminate in solutions containing calcium sulfate, J. Am. Ceram. Soc 67 (1984) 793–795.
[8] R.F. Feldman, V.S. Ramachandran, The influence of $CaSO_4.2H_2O$ upon the hydration character of $3CaO.Al_2O_3$, Mag. Concr. Res. 18 (57) (1966) 185–196.
[9] J. Skalny, M.E. Tadros, Retardation of tricalcium aluminate hydration by sulfates, J. Am. Ceram. Soc 60 (3–4) (1977) 174–175.
[10] D. Damidot, A. Nonat, P. Barret, Kinetics of tricalcium silicate hydration in diluted suspensions by microcalorimetric measurements, J.A.C.S. 73 (11) (1990) 3319–3322.
[11] D. Damidot, F.P. Glasser, Thermodynamic investigation of the $CaO–Al_2O_3–CaSO_4–H_2O$ system at 25 °C and the influence of Na_2O, Cem. Concr. Res., 23 (1) (1993) 221–238.
[12] H.N. Stein, Some characteristics of the hydration of $3CaO.Al_2O_3$ in the presence of $CaSO_4.2H_2O$, Sili. Ind. 25 (3) (1963) 141–145.
[13] H.F.W. Taylor, Cement Chemistry, Academic Press, 1990.